

Simple Phase-Space Trajectory Calculation for Monte Carlo Device Simulation Including Screened Impurity Scattering

F. M. Bufler, P. D. Yoder, and W. Fichtner

Institut für Integrierte Systeme, ETH Zürich
CH-8092 Zürich, Switzerland (E-mail: bufler@iis.ee.ethz.ch)

Abstract

A phase-space-step trajectory calculation within the scheme of self-scattering is presented. In addition, impurity scattering is approximated by the inverse microscopic relaxation time of the Ridley model. The resulting Monte Carlo algorithm is faster by a factor in the order of 15 than one, which integrates the equations of motion via a second-order Runge-Kutta technique and treats impurity scattering rigorously.

1. Introduction

As the characteristic length scales of MOSFETs continue to shrink, the device operation is more and more influenced by ballistic transport. Full-band Monte Carlo (FBMC) device simulation has been established as a reliable tool which can take this effect accurately into account. Since these simulations involve a large computational burden, it is important to improve their CPU efficiency. Progress in this direction was achieved by non-selfconsistent simulations where the electric field is taken from a drift-diffusion solution [1] or by efficient substrate current calculations [2]. Another promising approach consists of restricting the particles during the collisionless flight to one element of the phase-space [3] which enables e.g. to reduce the amount of self-scattering. On the other hand, impurity scattering is often neglected in FBMC device simulations [4, 5] to further save CPU time. However, the justification of this approximation is not clear in view of the high doping levels present in state-of-the-art devices. The aim of this paper is therefore twofold. On the one hand, the influence of impurity scattering on the dc output characteristics is investigated. On the other hand, an efficient implementation of impurity scattering within the 'phase-space step scheme' of Ref. [3] is presented together with some further general improvements of this approach.

2. Monte Carlo Model

The example chosen for the investigations is an $0.1 \mu\text{m}$ n-MOSFET the arsenic doping profile of which is displayed in Fig. 1. The grid of this 2D device consists of rectangles and triangles, and the Monte Carlo simulation is performed in a window containing

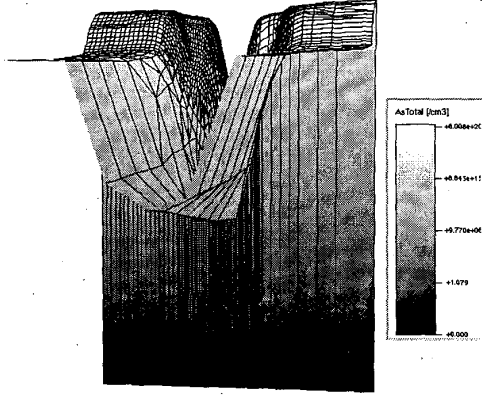


Figure 1: Arsenic doping profile of the 0.1 μm n-MOSFET

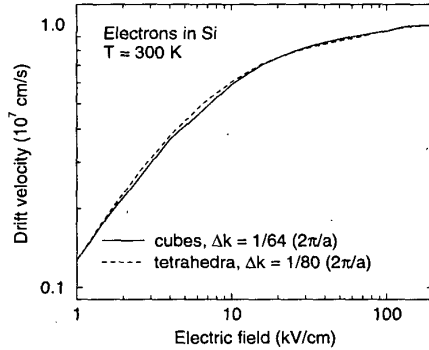


Figure 2: Influence of the k-space discretization on the velocity-field characteristics in undoped Si

1521 elements as described in [6]. The band and scattering model comprises the empirical pseudopotential band structure and phonon scattering described in Ref. [7] as well as impact ionization, impurity scattering and surface roughness scattering. The momentum space is discretized by an equidistant mesh of cubes with a spacing of $1/64 (2\pi/a)$ in all three coordinates, where a denotes the lattice constant, and the energy dispersion is linearly approximated within each cube. In Fig. 2, it is demonstrated that this mesh is fine enough by comparing the bulk velocity-field characteristic with the corresponding result of a finer mesh of tetrahedra for exactly the same physical situation (Fig. 5.25 on p. 119 of Ref. [7]).

3. Impurity scattering

The reason why scattering by screened ionized impurities involves such a large computational burden is that this process has a large scattering rate in the Brooks-Herring (BH) model, but leaves the particles' final state almost unchanged. Two reformulations of this scattering process help to enhance its CPU efficiency. First, substituting the BH model by the statistical screening model of Ridley (RI) [8] reduces the scattering rate significantly in some cases, of which a pronounced example is shown in Fig. 3 to emphasize this point. Second, the scattering rate can be replaced by the inverse microscopic relaxation time, when the momentum after scattering is chosen at random on the equienergy surface. This approximation has been shown to lead to almost the same results also in the nonlinear regime [9]. Finally, a doping-dependent prefactor of the rate is introduced in order to reproduce the experimental bulk mobility, especially at high doping levels [10]. While this approach is admittedly rather heuristic, it correctly accounts for the two main features, i.e. the strong mobility reduction in the highly doped contact regions and the screening in the inversion channel.

4. Phase-space trajectory calculation and simulation results

For the trajectory calculation of the particles the whole simulation time is divided into time intervals Δt . Within the interval, the time steps during which the particles

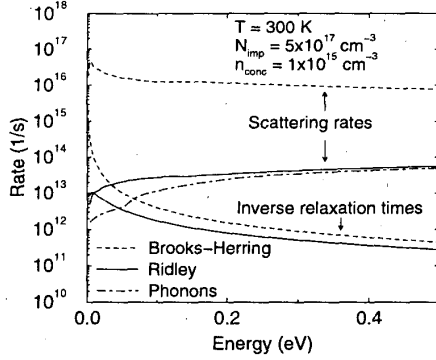


Figure 3: Scattering rates and inverse microscopic relaxation times of impurity scattering in the formulation of Brooks-Herring and Ridley. The phonon scattering rate is shown for comparison

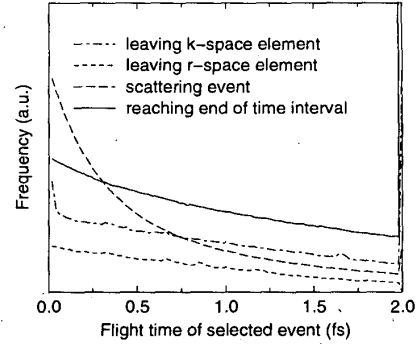


Figure 4: Frequency of the flight times of the *actually realized* events. Note that almost all particles do neither scatter nor change the phase-space element which could not be displayed in the figure.

are propagated according to Newton's law are determined such that the particle does not leave the phase-space element. These time steps are the minima of the times to leave the k -space element, to leave the r -space element, to reach the end of the time interval, and the stochastically chosen time of a real or fictitious scattering event. Note that in practice almost all particles reach the end of Δt without scattering or leaving the phase-space element. Among the several advantages are the simple integration of Newton's equations of motion, the restriction of actions (e.g. updating the group velocity) to the cases where it is necessary (in this example when the k -space element is left) and the possibility to assign to each phase-space element a relatively small constant upper estimation of the real scattering rate. Whereas upper estimations of the phonon and impact ionization scattering rates can be stored for each k -space element, impurity scattering depends also on density and doping. Therefore, an upper estimation is computed for each r -space element based on the density of the drift-diffusion solution and neglecting impurity scattering above 0.5 eV. A new advantage is the simple and relatively coarse mesh in k -space, because Fig. 4 shows that momentum-space changes occur rather often. Another new feature consists of mostly avoiding the costly computation of the logarithm in the self-scattering scheme. This is achieved by first considering the probability that scattering occurs before the three other possible events. The time of flight until a scattering event is only computed if this event is actually chosen.

Finally, the drain currents resulting from a FBMC device simulation with and without impurity scattering are shown in Figs. 5 and 6. It can be seen that impurity scattering has a non-negligible influence which can be mainly attributed to the mobility reduction in the highly doped contact regions.

5. Conclusions

In conclusion, we have shown by Monte Carlo device simulation that impurity scattering cannot be neglected for an accurate determination of drain currents in deep submicron MOSFETs. In addition, a speed-up of the Monte Carlo device simulation [6] by a factor in the order of fifteen was obtained by a simplified treatment of impurity scattering in combination with a simple phase-space trajectory calculation.

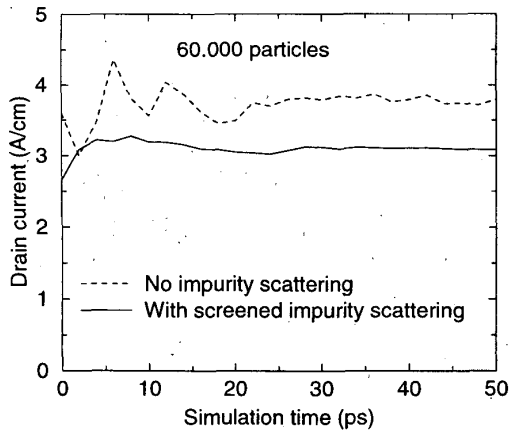


Figure 5: Drain current as a function of the simulation time for the bias point $V_{DS} = 0.3$ V and $V_{GS} = 2.3$ V

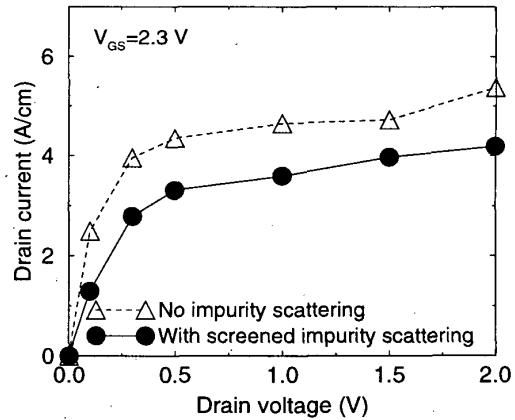


Figure 6: DC output characteristics of the $0.1 \mu\text{m}$ n-MOSFET with and without impurity scattering

References

- [1] J. M. Hgman, K. Hess, C. G. Hwang, and R. W. Dutton, "Coupled Monte Carlo-drift diffusion analysis of hot-electron effects in MOSFET's," *IEEE Trans. Electron Devices*, vol. 36, pp. 930–937, 1989.
- [2] C. Jungemann, S. Yamaguchi, and H. Goto, "On the accuracy and efficiency of substrate current calculations for sub- μm n-MOSFET's," *IEEE Electron Device Lett.*, vol. 17, pp. 464–466, 1996.
- [3] J. Bude and R. K. Smith, "Phase-space simplex Monte Carlo for semiconductor transport," *Semicond. Sci. Technol.*, vol. 9, pp. 840–843, 1994.
- [4] J. D. Bude and M. Mastrapasqua, "Impact ionization and distribution functions in sub-micron nMOSFET technologies," *IEEE Electron Device Lett.*, vol. 16, pp. 439–441, 1995.
- [5] S. E. Laux and M. V. Fischetti, "Monte Carlo study of velocity overshoot in switching a 0.1-micron CMOS inverter," in *IEDM Tech. Dig.*, 1997, pp. 877–880.
- [6] U. Krumbein, P. D. Yoder, A. Benvenuti, A. Schenk, and W. Fichtner, "Full-band Monte Carlo transport calculation in an integrated simulation platform," in *Proc. SISDEP*, Erlangen (Germany), Sept. 1995, pp. 400–403.
- [7] F. M. Bufler, *Full-Band Monte Carlo Simulation of Electrons and Holes in Strained Si and SiGe*. Munich: Herbert Utz Verlag, 1998 (<http://utzverlag.com>).
- [8] B. K. Ridley, "Reconciliation of the Conwell-Weisskopf and Brooks-Herring formulae for charged-impurity scattering in semiconductors: Third-body interference," *J. Phys. C*, vol. 10, pp. 1589–1593, 1977.
- [9] P. Graf, *Entwicklung eines Monte-Carlo-Bauelementsimulators für Si/SiGe-Heterobipolartransistoren*. Munich: Herbert Utz Verlag, 1999.
- [10] G. Masetti, M. Severi, and S. Solmi, "Modeling of carrier mobility against carrier concentration in arsenic-, phosphorus-, and boron-doped silicon," *IEEE Trans. Electron Devices*, vol. 30, pp. 764–769, 1983.